

# The Morphology of Poly(Vinylidene Fluoride) Crystallized from Blends of Poly(Vinylidene Fluoride) and Poly(Ethyl Acrylate)

ROBERT M. BRIBER<sup>†</sup> and F. KHOURY

Polymers Division, National Institute of Standards and Technology, Gaithersburg, Maryland 20899

## SYNOPSIS

A combined optical and electron microscopical study has been carried out of the crystallization habits of poly(vinylidene fluoride) (PVF<sub>2</sub>) when it is crystallized from blends with noncrystallizable poly(ethyl acrylate) (PEA). The PVF<sub>2</sub>/PEA weight ratios were 0.5/99.5, 5/95, and 15/85. Isothermal crystallization upon cooling the blends from the single-phase liquid region was carried out in the range 135–155°C, in which the polymer crystallizes in the  $\alpha$ -orthorhombic unit cell form. The 0.5/99.5 blend yielded multilayered and planar lamellar crystals. The lamellae formed at low undercoolings were lozenge shaped and bounded laterally by {110} faces. This habit is prototypical of the dendritic lateral habits exhibited by the crystals grown from the same blend at high undercoolings as well as by the constituent lamellae in the incipient spherulitic aggregates and banded spherulites that formed from the 5/95 and the 15/85 blends, respectively. In contrast with the planar crystals grown from the 0.5/99.5 blend, the formation of the aggregates grown from the 5/95 blend is governed by a conformationally complex motif of dendritic lamellar growth and proliferation. The development of these aggregates is characterized by the twisting of the orientation of lamellae about their preferential *b*-axis direction of growth, coupled with a fan-like splaying or spreading of lamellae about that axis. The radial growth in the banded spherulites formed from the 15/85 blend is governed by a radially periodic repetition of a similar lamellar twisting/fan-like spreading growth motif whose recurrence corresponds to the extinction band spacing. This motif differs in its fan-like splaying component from banding due to just a helicoidal twisting of lamellae about the radial direction. © 1993 John Wiley & Sons, Inc.

**Keywords:** banded • blend • spherulite • crystal • lamella • morphology • polymer • poly(ethyl acrylate) • poly(vinylidene fluoride) • splaying • twisting

## INTRODUCTION

This paper complements an earlier one<sup>1</sup> in which aspects of both the phase behavior of partially miscible blends of poly(vinylidene fluoride) (PVF<sub>2</sub>) with poly(ethyl acrylate) (PEA), as well as of the crystallization and morphology of the PVF<sub>2</sub> crystallized in the  $\alpha$ -crystal form<sup>2</sup> from such blends, were reported. The phase diagram of the PVF<sub>2</sub>/PEA blend system shown in Figure 1 has been described and discussed in the previous paper,<sup>1</sup> which also in-

cluded the results of a study of the kinetics of  $\alpha$ -PVF<sub>2</sub> spherulite growth from the homogeneous liquid phase (see Figure 1) in blends in which the PVF<sub>2</sub>/PEA weight ratio was in the range 10/90 to near 50/50. The description of the morphology of the spherulites reported in the same paper was limited to observations on the gross texture of the  $\alpha$ -spherulites using light optical microscopy. The aspects of the morphology of the spherulites pointed out were the increased openness of the texture of the spherulites with decreasing PVF<sub>2</sub> concentration as evidenced by using phase contrast optics, and the systematic effects of crystallization temperature and PVF<sub>2</sub> concentration on the spatial periodicity of the annular banding (extinction rings) exhibited by the spherulites when observed between crossed polarizer

<sup>†</sup> Current address: Department of Materials Science and Engineering, University of Maryland, College Park, MD 20742-2115.  
Journal of Polymer Science: Part B: Polymer Physics, Vol. 31, 1253–1272 (1993)  
© 1993 John Wiley & Sons, Inc. CCC 0887-6266/93/101253-20

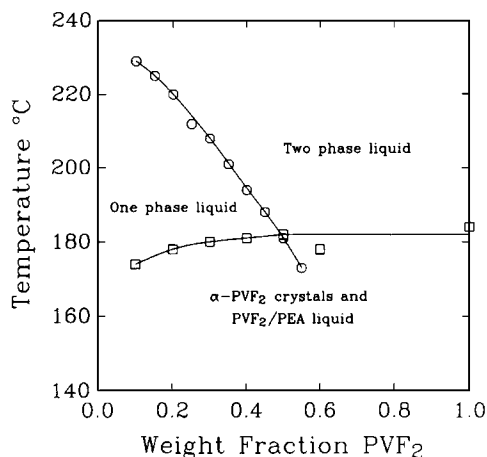


**Figure 1.**  $\alpha$ -PVF<sub>2</sub>/PEA-phase diagram,<sup>1</sup> cloud points (circles); equilibrium melting points (squares).

and analyzer.<sup>1</sup> Recapitulating the latter results, it was found that for a given PVF<sub>2</sub> concentration the separation between the bands increased with increasing crystallization temperature. This parallels the effect of crystallization temperature on the band spacing in  $\alpha$ -spherulites grown in undiluted PVF<sub>2</sub>,<sup>3</sup> and from PVF<sub>2</sub>/poly(methyl methacrylate) (PMMA) blends,<sup>4</sup> as well as melt-grown banded polymer spherulites generally.<sup>5a</sup> In addition, as is the case for the PVF<sub>2</sub>/PMMA blends,<sup>4</sup> the band separation in the  $\alpha$ -spherulites grown from the PVF<sub>2</sub>/PEA blends at a given crystallization temperature increased with decreasing PVF<sub>2</sub> concentration.

In the present article the results of a combined light optical and electron microscopical study of the crystallization habits exhibited by PVF<sub>2</sub> crystallized in the  $\alpha$  form isothermally from blends in which the PVF<sub>2</sub>/PEA weight ratios were 0.5/99.5, 5/95, and 15/85 are described and discussed. In all the experiments, crystallization was carried out upon cooling the blends from the single phase liquid region (see phase diagram, Figure 1) directly to temperatures in the range of 135–155°C. Crystallization from the 0.5/99.5 blend yielded multilayered and conformationally planar lamellar crystals. Incipient spherulitic aggregates and banded spherulites were formed from the 5/95 and the 15/85 blends, respectively. The main novel features of the morphology of  $\alpha$ -PVF<sub>2</sub> described and discussed in the present study are the following: (a) The related lateral growth habits of the constituent lamellae in the crystals, aggregates, and spherulites differ distinctly from the previously reported quasi-hexagonal lateral habits exhibited by  $\alpha$  crystals grown from dilute solutions

of PVF<sub>2</sub> in 9 : 1 mixtures of monochlorobenzene and dimethyl formamide.<sup>6-9</sup> (b) The morphological evolution of the aggregates formed from 5/95 blends is governed by a conformationally complex type of growth motif characterized by an effective twisting of the orientation of lamellae about the *b*-crystallographic axis coupled with a fan-like splaying or spreading of lamellae about that axis. The radial propagation of growth in the banded spherulites grown from 15/85 blends is governed by a periodic repetition of a similar lamellar twisting/splaying type of growth motif.

## EXPERIMENTAL

The PVF<sub>2</sub> was obtained from the Soltex Corporation and carried the designation XP8N.<sup>10</sup> This is a relatively low molecular weight PVF<sub>2</sub> with  $M_n = 47,000$  and  $M_w/M_n = 2.7$  as measured by gel permeation chromatography (GPC) by the manufacturer. The PEA was purchased from Scientific Polymer Products<sup>10</sup> and had  $M_n = 29,000$  and  $M_w/M_n = 2.4$  as measured by GPC by the manufacturer. The blends were prepared by first dissolving the polymers in the desired weight ratio in dimethyl formamide (DMF) at room temperature and at a blend concentration of about 5% and then rapidly precipitating the polymers by pouring the solution in water. Following the notation adopted in the Introduction, the blend compositions in the remainder of the paper are expressed in terms of PVF<sub>2</sub>/PEA weight ratios.

The precipitated blends were dried for up to a week in a vacuum oven at room temperature. By preparing the blends in this manner, initially homogeneous samples were obtained. If the blends were prepared by solution casting rather than precipitation, the PVF<sub>2</sub> tended to crystallize out in the form of large spherulites, thereby generating local concentration gradients of PVF<sub>2</sub> that persisted in the films even after melting. Film casting was therefore not adopted. Unless stated otherwise, all the specimens were crystallized using the following procedure: Once a blend of the desired concentration was prepared, a small portion of the precipitated and dried material was melted on a glass slide placed on a hot plate at a temperature of about 225°C for the samples with a cloud point  $T_{cl} > 225^\circ\text{C}$  and at a temperature of about  $T = T_{cl} - 10^\circ\text{C}$  for the blends with higher PVF<sub>2</sub> content (see Figure 1). Once the blend was melted, a coverslip was placed over the sample on the glass slide, which was then inserted in a Mettler FP-2 hot stage<sup>10</sup> preset and controlling at the desired crystallization temperature. The films

formed in this manner were 10–20- $\mu\text{m}$  thick. Crystallization, which was monitored with a light microscope using phase contrast optics, was generally allowed to proceed to completion, although in some cases, where the early stages of spherulite development were of interest, the samples were quenched to room temperature at intermediate stages of crystallization by removing them and placing the slide on a room temperature metal block. This quenching procedure was also used at the end of experiments, which were carried out to completion of crystallization.

For the transmission, scanning transmission, and scanning electron microscopy studies (TEM, STEM, and SEM, respectively), sample preparation necessitated the removal of the top coverslip and then the dissolving away of the PEA. The coverslip was easily removed by immersing the slide in liquid nitrogen gradually (so as not to crack the glass) whereupon due to the contraction of the polymer, the coverslip would usually detach itself and fall off. The glass slide supporting the PVF<sub>2</sub>/PEA specimen was then placed in a Soxhlet extractor and refluxed for 2–3 h with acetone, which is a good solvent for the PEA and a nonsolvent for PVF<sub>2</sub>. In the refluxing process PVF<sub>2</sub> crystals, incipient spherulites or spherulites that were not attached to the surface of the glass slide were washed away, but enough material remained attached to allow morphology studies. For SEM the glass slide was sputter coated with gold and examined directly, while for TEM detachment replicas were made as follows. The PVF<sub>2</sub> structures on the glass slide were first shadowed with 80/20 Pt/Pd alloy at an angle of  $\tan^{-1}(1/3)$ . A thin (10-nm) coating of amorphous carbon was then evaporated onto the shadowed specimen, which was then coated with a 2% polyacrylic acid (PAA)/water solution. Once dry, the PAA was peeled away. This resulted in the removal of the carbon–Pt/Pd–PVF<sub>2</sub> sandwich (attached to the PAA) from the glass slide. The PAA–carbon–Pt/Pd–PVF<sub>2</sub> composite was then cut into squares that were placed on electron microscope grids, and the PAA dissolved and washed off with distilled water. The PVF<sub>2</sub> was then dissolved away (the objects of interest were usually too thick for electron beam transmission) with DMF at room temperature, leaving behind only the carbon film backed Pt/Pd replica. In a few cases for the more dilute PVF<sub>2</sub> blends the PVF<sub>2</sub> was not dissolved away thus allowing the direct examination of the objects (crystals) of interest as well as the acquisition of selected area electron diffraction patterns.

The scanning electron microscopy was performed using an ETEC U-1 Autoscan microscope.<sup>10</sup> The

transmission electron microscopy was performed using both Philips 300 and 400T microscopes<sup>10</sup> operated at 80 and 100 KV respectively. Both microscopes were equipped with STEM units.

## RESULTS

The experimental observations on the crystallization habits exhibited by PVF<sub>2</sub> crystallized from the 0.5/99.5, 5/95, and 15/85 PVF<sub>2</sub>/PEA blends are described separately in the three ensuing subsections in that order.

### The Morphology of Crystals Grown from 0.5/99.5 Blends at 150 and 135°C

The PVF<sub>2</sub> crystallized at 150°C in the form of multilayered lamellar single crystals whose constituent lamellae are about 10-nm thick and are typically lozenge shaped. This latter feature, as well as the multilayered character of the crystals, may be seen in the TEM picture of the replica shown in Figure 2, in which several crystals are exhibited. As visible in this figure, the development of layers in the crystals occurs through the agency of screw dislocations. The lamellae are apparently flat as grown. They do not exhibit any of the features, such as pleats or ridges, usually associated with the flattening of non-planar (e.g., hollow pyramidal) polymer crystals on a planar substrate upon drying from suspension in

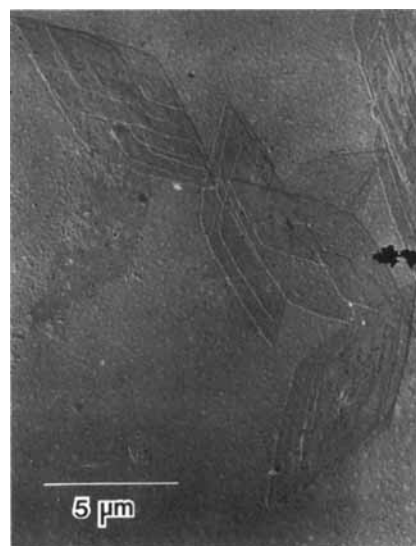


**Figure 2.** Transmission electron micrograph of a replica of several crystals of PVF<sub>2</sub> grown at 150°C from a 0.5/99.5 blend.

liquid. Electron diffraction patterns obtained from crystals from the same crystallization experiment, but in which case the PVF<sub>2</sub> was not dissolved away with DMF, corresponded to the  $hk0$  reciprocal lattice net of  $\alpha$ -PVF<sub>2</sub>, which indicates that the stems of the constituent folded molecules are oriented at right angles to the plane of the lamellae. Figure 3a is a STEM picture of a multilayered crystal. The corresponding electron diffraction pattern obtained from an area of the crystal approximately 0.5  $\mu\text{m}$  in diameter with the incident electron beam normal to the lamellae is shown in Figure 3b, in which it is indexed according to the  $\alpha$ -crystal form.<sup>2</sup> The critical feature identifying the diffraction patterns exhibited by the crystals as of the  $\alpha$  form as distinct from the  $\gamma$  form<sup>11-13</sup> is the presence of 100 reflections, which are forbidden in the latter form. In addition to establishing that the unit cell structure is the  $\alpha$  form, the diffraction data show that the long and short axes of the lozenges are parallel to the  $b$  axis and to the  $a$  axis of the unit cell, respectively, and that the lateral growth faces of the lamellae are  $\{110\}$ .

The lateral growth habit of the crystals described above differs distinctly from previously reported habits of  $\alpha$ -PVF<sub>2</sub> crystals grown from dilute solutions of the polymer in 9 : 1 monochlorobenzene/dimethylformamide mixtures. The  $\alpha$  crystals re-

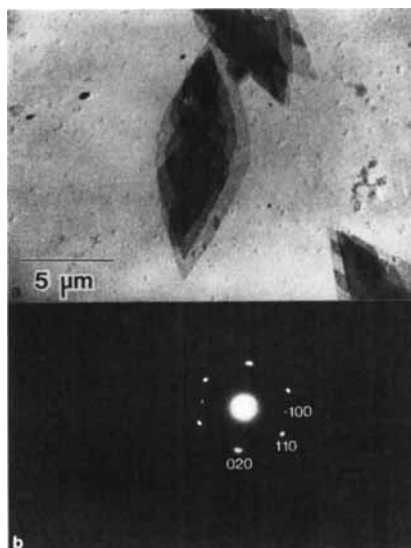


**Figure 3.** (a) Scanning transmission electron micrograph of a multilayered PVF<sub>2</sub> crystal grown at 150°C from a 0.5/99.5 blend. (b) Electron diffraction pattern obtained from an area about 0.5  $\mu\text{m}$  in diameter in the lower part of the crystal. The pattern is indexed according to the  $\alpha$ -crystal form of PVF<sub>2</sub>.<sup>2</sup> Note the presence of 100 reflections (see text).

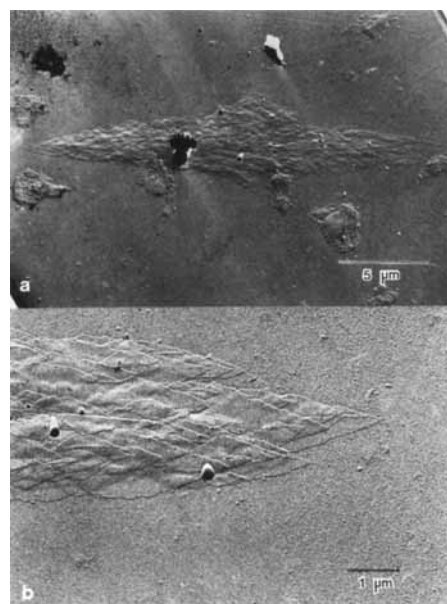


**Figure 4.** (a) Transmission electron micrograph of a replica of a multilayered dendritic crystal of PVF<sub>2</sub> grown from a 0.5/99.5 blend at 135°C. (b) A view at higher magnification of part of another dendritic crystal.

ferred to are those grown by Okuda et al.,<sup>6</sup> Grubb et al.,<sup>7,8</sup> and Lovinger,<sup>9</sup> who have described lamellae that either exhibited rounded overall profiles with no well-defined or distinguishable lateral faceting, or that exhibited “quasi-hexagonal” lateral shapes corresponding in essence to truncated lozenges bounded laterally by  $\{110\}$  and  $(020)$  faces,<sup>6-9</sup> albeit with the corners between faces being variously rounded. As will be seen from the experimental results described in the remainder of this paper, no instances were observed in the present study of the development of  $(020)$  faces in  $\alpha$  lamellae grown from the PVF<sub>2</sub>/PEA blends.

Crystallization at 135°C from 0.5/99.5 blends yielded multilayered dendritic crystals in which the lateral growth habit of the constituent lamellae derives from the lozenge habit of the crystals described above. Figure 4a is a transmission electron micrograph of a replica of an entire crystal. A view at higher magnification of a portion of another dendritic crystal is shown in Figure 4b. It is common experience in the crystallization of polymers from dilute solutions that diffusion becomes a factor controlling lamellar grow at high undercoolings, and that the nucleation of new fold planes (i.e., the formation of new strips of folded molecules) at the periphery of lamellae is favored at protruding corners (see ref. 5b for a brief review). When the basic habit

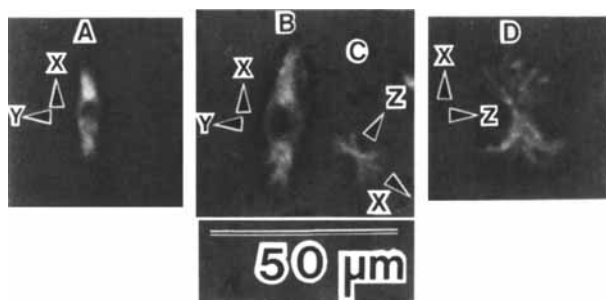


**Figure 5.** Phase contrast light optical micrographs illustrating the difference in the appearance exhibited by aggregates formed in a 5/95 blend at 155°C when seen in different perspectives while still embedded in PEA. Z projection, aggregates A and B; Y projection, aggregates C and D (see text).

of the lamellae is lozenge-like, as is the case for PVF<sub>2</sub> in the present circumstances, the nucleation of new strips is all the more favored at the acute corners. This results in an enhancement of growth in the direction parallel to the long axis of the basic lozenge, which is the *b* axis in the present instance. Preferential nucleation at protruding corners leads to the development of sectored outgrowths<sup>5b</sup> entailing reentrant {110} microfaceting. This latter feature is evidenced by the serrated nature of the lateral edges of lamellae as can be seen in the higher magnification micrograph shown in Figure 4b. The incipient spiraling development of lamellar overlayers from screw dislocations in underlying layers may also be observed in the latter micrograph. The appearance of the crystals in the films as observed with a phase contrast light microscope prior to the removal of the PEA, as well as the electron microscopical observations (Figure 4), indicated that the overall conformation of these crystals is planar. In anticipation of what follows, it is pertinent to indicate that this planarity contrasts with the distinctly nonplanar conformations exhibited by the aggregates formed in films of the 5/95 blends, which are described in the next subsection. As a further check that the overall conformation of the aforementioned dendritic crystals is planar, an additional experiment was performed in which crystallization was carried out at 135°C in a bulk sample of the 0.5/99.5 blend about 2-mm thick held in the bottom of a test tube whose diameter was about 0.5 cm. After crystallization was completed and the sample quenched, the PEA was dissolved away by repeated washings with hot acetone without allowing the preparation to dry between washings. Examination of the crystals in suspension in acetone as they tum-

bled in the field of view of a phase contrast light microscope confirmed that even when grown in bulk, where limitation to development in the specimen film thickness direction does not arise, their overall as-grown conformation was also planar.

#### The Morphology of Crystalline Aggregates Formed from 5/95 Blends at 155 and 145°C

Crystallization even at the highest temperature ( $T_c = 155^\circ\text{C}$ ) that was probed at this blend composition resulted in the formation of multilayered crystalline aggregates, which exhibited pronounced conformational deviations from the planar overall conformation exhibited by the crystals described in the previous section. The aggregates were randomly oriented relative to the plane of the films in which they grew. It was thus possible from a consideration of their appearances in different orientations to “reconstruct” in broad outline the salient features of their three-dimensional development from an initial examination of the films at  $T_c$  or after quenching, using phase contrast light microscopy. More detailed examinations of the variously oriented aggregates that remained stuck to the glass substrate after the PEA was washed away were then carried out using SEM.

Figures 5–8, which include both light and scanning electron micrographs, serve to illustrate the salient characteristics of the development and morphology of the type of aggregates formed at 155°C. The particular preparation from which these micro-

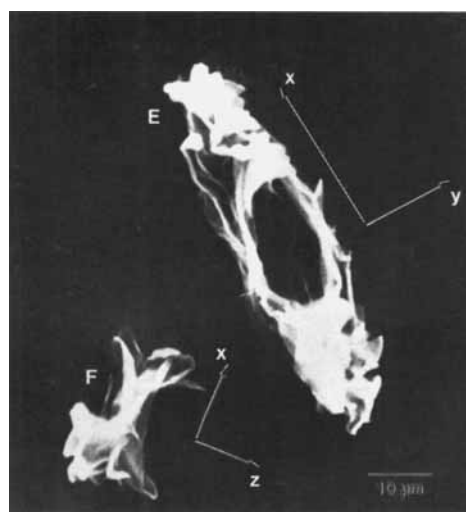


**Figure 6.** Scanning electron micrograph of two aggregates grown in a 5/95 blend at 155°C. (Z projection, aggregate E; Y projection, aggregate F; see text).

graphs were taken had been kept at the crystallization temperature for five days prior to quenching. By that time the aggregates had stopped growing. There were some random variations in the sizes of the aggregates, indicating that some had started to grow later than others.

The light optical micrographs in Figure 5, in which aggregates still embedded in PEA are shown, illustrate the contrasting appearances exhibited by the aggregates when viewed in two main projections at right angles to one another. Using as reference the roughly acicular lateral profiles exhibited by the aggregates in the projection represented by objects A and B in Figure 5, then the orientational relationship between the habit exhibited by the aggregates in that projection with that represented by objects C and D in the same figure is as follows. Denoting the long and short axes of objects A and B as the  $X$  and  $Y$  axes of the aggregates, respectively, and the axis normal to the  $XY$  plane as  $Z$ , then objects C and D represent aggregates viewed in projection along the  $Y$  axis. In the latter perspective they characteristically exhibit an overall sheaf-like appearance.

It is evident from the distinctly different profiles exhibited by the aggregates in the two perspectives described above that the  $X$  axis is not an axis of cylindrical symmetry. The overall sheaf-like pattern of propagation is clearly preferentially restricted to growth in the  $XZ$  plane. Accordingly, when viewed along the  $Z$  axis the aggregates are effectively thinner at the center than further out in opposite directions along the  $X$  axis. This accounts for the differences in contrast seen between the corresponding regions in aggregates A and B in Figure 5.

Turning to the scanning electron micrographs shown in Figures 6–8, it should be noted that

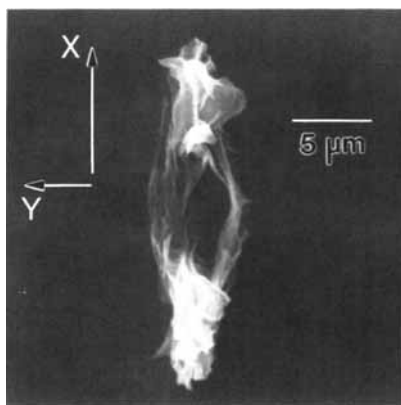


**Figure 7.** Scanning electron micrograph of an aggregate grown from a 5/95 blend at 155°C ( $Z$  projection).

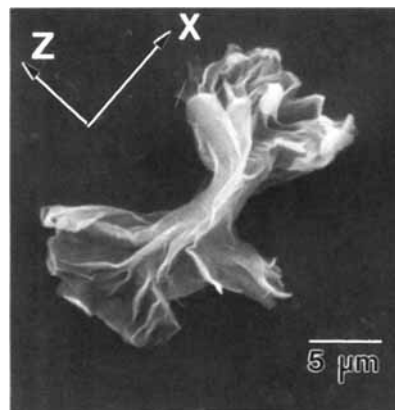


**Figure 8.** Scanning electron micrograph of an aggregate grown from a 5/95 blend at 155°C ( $Y$  projection).

whereas the aggregates shown therein had not undergone any evident distortions upon exposure to the electron beam, the occurrence of some distortions during the washing and drying operations involved in the removal of the PEA is likely. While details of the lamellar organization in these objects remain to be elucidated, examination in the SEM nevertheless reveals some main features of the nature of their morphological development that are consistent with and complement the light microscopical observations described above on the aggregates still embedded in PEA.

When viewed in the  $Z$  projection in the SEM, the aggregates exhibit an overall appearance that may be roughly described as “boat-like,” as can be seen in Figure 6 (object E) and Figure 7. As expected, they appear sheaf-like when viewed in the  $Y$  projection (Fig. 8 and object F in Figure 6). The acicular character of the profile of the aggregates in the  $Z$  projection suggests in itself that the basic lateral growth habit of the constituent lamellar layers in the aggregates derives from the habit of the lozenge-shaped crystals (or the related dendritic crystals) grown from the 0.5/99.5 solutions, and that the preferential direction of growth of the lamellae is in the  $b$ -axis direction. In contrast with the crystals grown from the more dilute blend, however, the growth and proliferation of the lamellae underlying the formation of these aggregates are characterized by pronounced conformational deviations from planar propagation. The nature of these deviations is examined and discussed further below.

The sheaf-like character exhibited by the aggregates when viewed along the  $Y$  axis, coupled with their centrally recessed boat-like appearance in the  $Z$  projection, may be adduced as evidence that in

the central region the conformation of the objects approximates that of two round-bottomed (keel-less) boats set together hull bottom to hull bottom. The elongated and pronouncedly dished character of the central region of the boat-like halves of the aggregates indicates that conformational curvature involving an element of curling about the  $X$  axis is a dominant feature of the growth and propagation of the lamellar envelope in that region. A tentative representation of the cross section of the envelope parallel to the  $YZ$  plane at the *center* of the aggregates is illustrated in Figure 9, where the extent of curling between the central and the rim regions of the recessed interior portion of the aggregates is depicted to be  $90^\circ$ . Its tentative nature notwithstanding, this diagrammatic representation of the conformation of the  $X$ -axis projection of the lamellar envelope at the *center* of the aggregates serves as a useful base of departure in considering the conformation details of the morphological development of the aggregates beyond the central region and toward the opposite extremities along the  $X$  axis.

The appearance of the aggregates as viewed in the  $Z$  projection (E in Fig. 6, Fig. 7) indicates that the curling of the lamellar envelope about the  $X$  axis occurs well beyond the central region. Proceeding progressively beyond the aggregate center toward both extremities in the  $X$  direction, opposite parts of the envelope, which surrounds the central recessed interior region, converge progressively toward one another until they seemingly merge. This apparent converging and merging of the sides of the lamellar envelope situated on opposite sides of the  $X$  axis as growth progresses in the  $X$  direction, occurs in association with the overall fan-like propagation of growth preferentially parallel to the  $XZ$  plane beyond the central region (Figures 5D and 8).

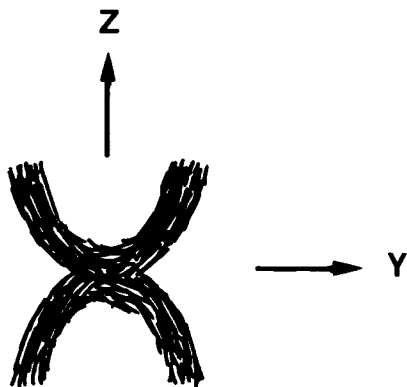


**Figure 9.** Schematic representation of the apparent  $XZ$  cross-section of the lamellar envelope at the *center* of the aggregates formed at  $155^\circ\text{C}$  from 5/95 blends.

Given the likelihood of distortions incurred during washing and drying, extraction of more information (from the scanning electron micrographs) on the growth and conformational details of the emergence of the latter pattern of propagation beyond the central region is obviously subject to uncertainties. Nevertheless, the micrographs strongly suggest that the fan-like spreading of lamellar layers preferentially in the  $XZ$  plane and with their fold surfaces preferentially parallel to that plane are dominant features of the propagation of growth beyond the central region of the aggregates. This feature entails *in effect* a twisting change in the orientation of the plane of lamellae through about  $90^\circ$  about the  $X$  axis between that at the very center of the aggregate and that at each of its extremities along  $X$ .

Crystallization at  $145^\circ\text{C}$  from the 5/95 blends yielded aggregates of varying complexity. The light optical micrograph shown in Figure 10 illustrates several aggregates grown in a film (over a period of several days) as they appear after the PEA was washed away. A few of these aggregates (for example G, H, I) exhibit simpler overall sheaf-like appearances characterized by a pronounced fan-like spreading of the constituent structural units at opposite extremities of the central sheaf axis. Similar fan-like propagation of growth is also observed at the extremities of the branches radiating from the center of the more complex aggregates (for example Figure 10, aggregate J).

It should be noted, in anticipation of the electron microscopic observations described below, that in some instances aggregates formed at  $145^\circ\text{C}$  were observed with phase contrast light microscopy to exhibit during their early stages of growth an appearance resembling that exhibited by the aggregates grown at  $155^\circ\text{C}$  as viewed in the  $Z$  direction while still embedded in the PEA (Figure 5). Other aggregates were seen to exhibit a sheaf-like appearance. In short, it appears that the aggregates formed at  $145^\circ\text{C}$  evolve from precursors that are morphologically similar or related to the aggregates formed at  $155^\circ\text{C}$  described above.

Transmission electron micrographs of surface replicas of aggregates, or parts of aggregates, formed in the same preparation as those in Figure 10 are shown in Figures 11–13. Two features exhibited in these micrographs may be noted from the outset. First, the similarity between the lateral growth habit of the constituent lamellae in these aggregates and that of the dendritic crystals grown from the 0.5/99.5 blends clearly indicates that the preferential direction of growth in individual lamellae is the  $b$  axis. The second feature is the fan-like splaying of

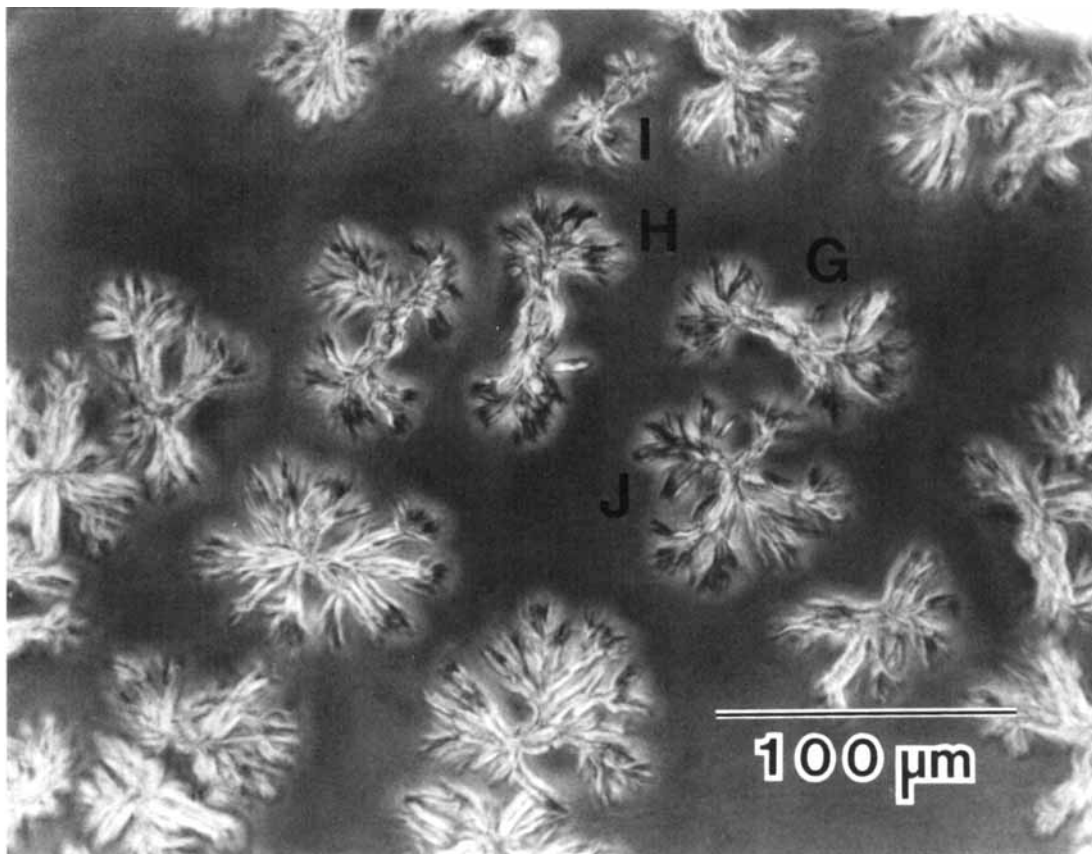


**Figure 10.** Phase contrast light optical micrograph of aggregates grown from a 5/95 blend at 145°C as they appear after the PEA has been washed away.

lamellae at the extremities of the aggregates. This latter feature may be seen at opposite extremities of the long central axis of the sheaf-like aggregate shown in Figure 11. It is also evident in Figure 12c, which is a higher magnification micrograph of a portion of Figure 12a. The latter figure encompasses the central region and one extremity along the long axis of an aggregate. A similar fan-like spreading or splaying of lamellae may also be seen in Figure 13 in which a “branch” of one of the more complex quasi-radiating species of object (akin to object J, Figure 10) is shown. The salient features just described are examined and discussed further below in association with additional details of the lamellar organization in the aggregates as seen in the replicas.

Pronounced ridge-like features, which may be traced from the interior of the aggregates outwards to fan-like splayed lamellae (or stacks of lamellae) lying flat on the substrate at the extremities of the aggregates, may be seen in Figures 11–13. The considerable elevations of the ridges relative to the substrate and the lamellae lying flat on it at the aggregate extremities in each of these replicas, and all

others that have been examined, is evidenced by the wide shadows they exhibit. Upon close examination it is found that these ridges are associated with pronounced changes in the inclination of stacked la-

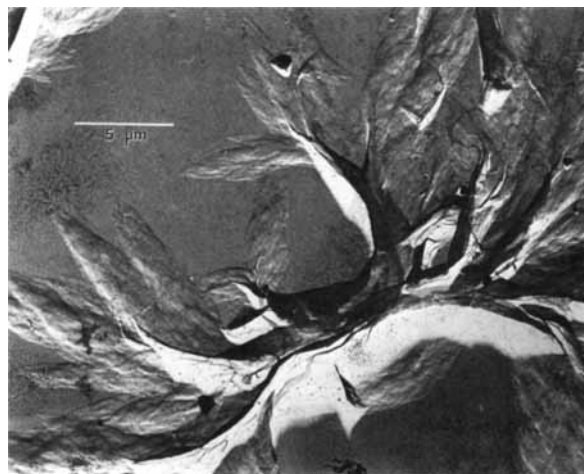


**Figure 11.** Transmission electron micrograph of a replica of an aggregate grown from a 5/95 blend at 145°C.

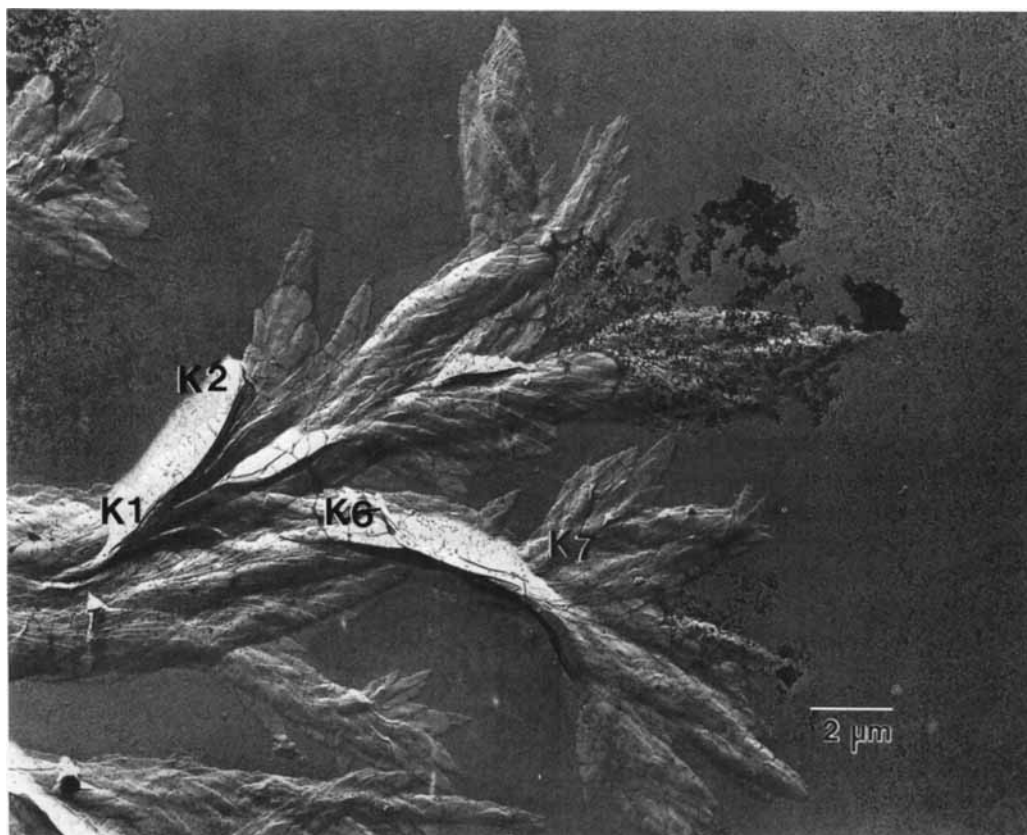


**Figure 12.** (a) Transmission electron micrograph of a replica of part of an aggregate grown from a 5/95 blend at 145°C. (b) and (c) Views at a higher magnification of parts of (a). See text for the description of and comments on the annotated features.

mellae, from being oriented preferentially edge-on, to essentially flat-on (relative to the substrate) along their outward propagation direction. Referring for example to Figure 12 in this connection, attention is drawn to the magnified views in Figure 12b,c of two elevated ridges in the aggregate shown in Figure 12a whose central region lies at the bottom left-hand corner of the latter micrograph. These two ridges, denoted K1-K2 and K6-K7, respectively, are considered in that order below.

Considering Figure 12b, attention is drawn to the windward side (relative to the shadowing direction) of ridge K1-K2, where closely bunched edges of lamellae can be seen to diverge progressively away from and to the right of the sharply defined ridge near which the lamellar orientation is preferentially at right angles to the substrate. To varying extents, the edges of the lamellae are traceable from the vicinity of the ridge toward the outer regions denoted K3 and K4 where the lamellae lie parallel to the substrate. Turning to Figure 12c, it may be seen that ridge K6-K7 is a central feature associated with the

development of a seemingly distinct "branch" of the sheaf. This branch, which emerges from the stack of lamellae in region K5 to the left of the ridge, appears narrower in projected width alongside the midsection of the ridge between K6 and K7, and culminates at its outer extremity in a fan-like splaying of lamellae (denoted K8) that lie parallel to the substrate. The edges of some of the lamellae in the latter region can be traced to the crest of the ridge near K7. These various topographical characteristics, considered collectively, can be reasonably taken as evidence that in the region immediately adjoining the crest along K6-K7 the constituent lamellae in the diverging branch are oriented edge-on relative to the substrate. This is in marked contrast with lamellae K8, which are spread flat-on at the outer extremity of the branch, as well as with the lamellae in and around region K5 where, even though they appear variously inclined relative to the substrate, they are far from being oriented edge-on to it. Kindred examples of ridge-associated changes in the orientation of the plane of lamellae or stacks of la-

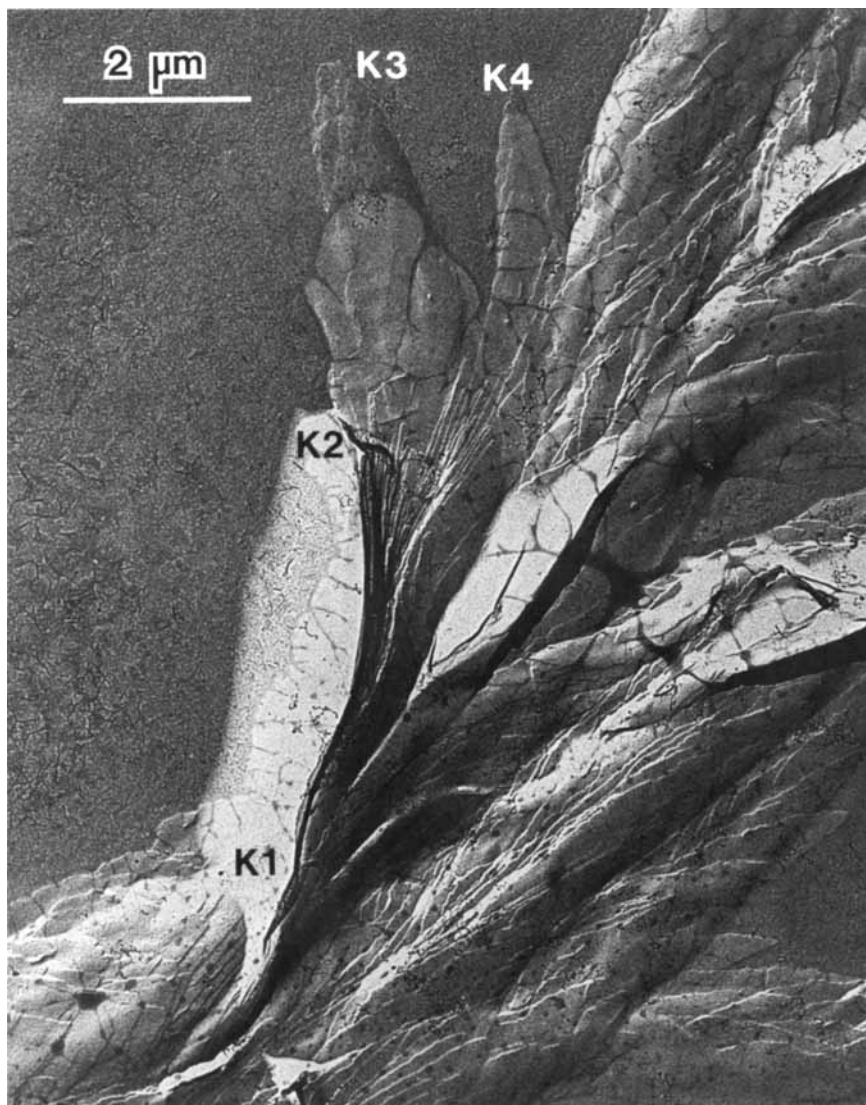
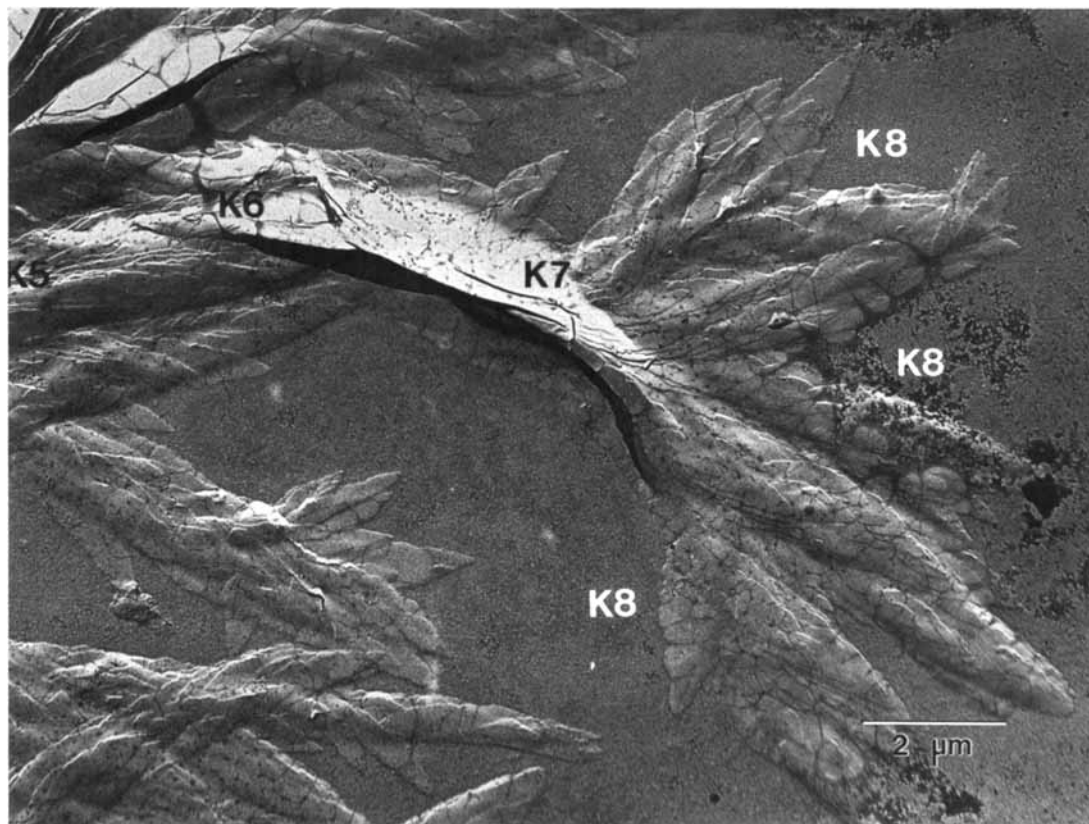


Figure 12 (continued from the previous page)

mellae, seemingly involving a twisting about their outward direction of propagation, and culminating in a fan-like spreading of lamellae, may be seen about the replicas in Figures 11–13.

The possibility that the complex aggregates formed at 145°C may undergo distortions upon drying following extraction of the PEA with acetone cannot be ruled out. The observations described above indicate that an apparent twisting in the orientation of interleaved lamellae about the *b* axis, in association with a fan-like spreading of lamellae, are dominant features of the morphological evolution of these aggregates. The genuineness of these features as being associated characteristics of the aggregates as grown is indicated by their apparent

kinship to the propagational characteristics exhibited in the SEM by the fairly rigid aggregates formed at 155°C. This view is reinforced by the observation, indicated earlier prior to the description of Figures 11–13, that aggregates formed at 145°C were observed to in the light microscope to evolve from precursors that are apparently similar or related to the aggregates formed at 155°C. As will be seen below, kindred growth characteristics, but involving the periodic repetition of lamellar twisting in association with fan-like splaying or spreading, underlie the banding in spherulites grown from blends containing a higher concentration of PVF<sub>2</sub>. In other words, these aggregates grown at 155 and 145°C from the 5/95 blends contain the structural elements that



**Figure 12** (continued from the previous page)

lead to the banding in spherulites grown from blends with higher PVF<sub>2</sub> concentration.

#### The Morphology of Banded Spherulites Grown from 15/85 PVF<sub>2</sub>/PEA Blends

A description is presented in this section of the morphological characteristics that underlie the manifestation of banding in PVF<sub>2</sub> spherulites grown from 15/85 PVF<sub>2</sub>/PEA blends at 150 and at 145°C in which the band spacings were approximately 30 and 25 μm, respectively. The observations that are reported below stem from an examination of the spherulites after the PEA was washed away from the films in which they were formed. A feature of the radial propagation of growth in the spherulites is the periodic recurrence of “spurts” of fan-like lamellar splaying about the radial direction of growth at intervals corresponding to the radial periodicity of the banding. As will be seen, this recurring pattern of branching bears similarities to the twisting/fan-like splaying features encountered in the aggregates formed from the 5/95 blends.

The observation that radially periodic spurts of divergent branching underlie the banding in the

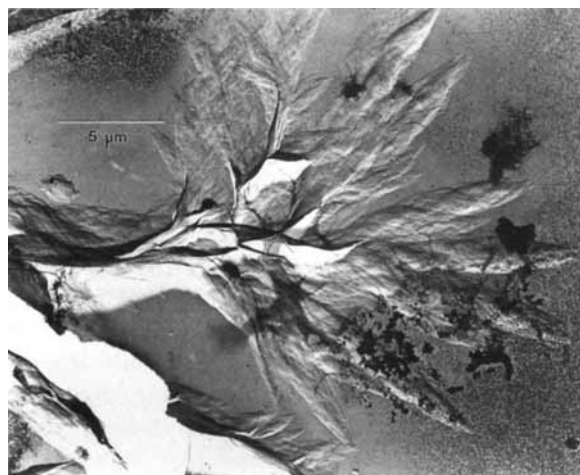


**Figure 13.** Transmission electron micrograph of the replica of part of a radiating species of aggregate (similar to aggregate J in Figure 10) grown from a 5/95 blend at 145°C.

spherulites grown from this blend at 150°C was first clearly brought into evidence upon examination of spherulites with a light optical microscope, using phase contrast optics, after the PEA was washed away. The morphological details underlying the manifestation of this branching (which is not clearly evident in phase contrast optical micrographs of these spherulites still embedded in PEA, see Fig. 8i, in ref. 1) were then probed directly in a SEM. Replicas of the spherulites were also prepared and examined in a TEM.

It should be noted in connection with the ensuing observations that a spatially periodic occurrence of fan-like branching that coincides with the periodicity of the banding is readily distinguishable with phase contrast light microscopy prior to the washing away of the PEA in banded spherulites grown from blends having higher PVF<sub>2</sub> concentrations than 15/85 (e.g., 25/75, 35/65, see Figs. 8e and 8g in ref. 1). Periodic spurts of fan-like branching are a genuine growth feature of banded PVF<sub>2</sub> spherulites grown from PVF<sub>2</sub>/PEA blends. This feature has been observed (prior to removal of the PEA) in banded spherulites formed in films crystallized between glass surfaces as well as films crystallized with a free surface.

Figure 14a is a phase contrast light micrograph illustrating spherulites grown at 150°C from a 15/85 blend as they appear after the PEA has been washed away. The smaller structure in Figure 14a is a relatively immature spherulite. A view at higher magnification of one of the spherulites in Figure 14a is shown in Figure 14b.

As can be seen in Figure 14a, and in more detail in the view at higher magnification shown in Figure 14b, the manifestation of spurts of fan-like microbranching underlies the radial proliferation of growth in these spherulitic structures. The emergence of these fan-like arrangements of lamellae from narrow radially oriented stem-like growth features, which themselves emerge from a preceding spurt, can be discerned in many instances both at the periphery and in the interior of the spherulites. In addition, a radial periodicity of about 30 μm between successive spurts of fan-like branching can be seen about the spherulites. The scanning electron micrograph of a portion of the periphery of a spherulite grown at 150°C that is shown in Figure 15 illustrates the qualitative similarity between the manifestation of fan-like branching in these spherulites and the fan-like spreading of lamellae encountered earlier at the extremities of the aggregates grown from 5/95 blends (see previous section).

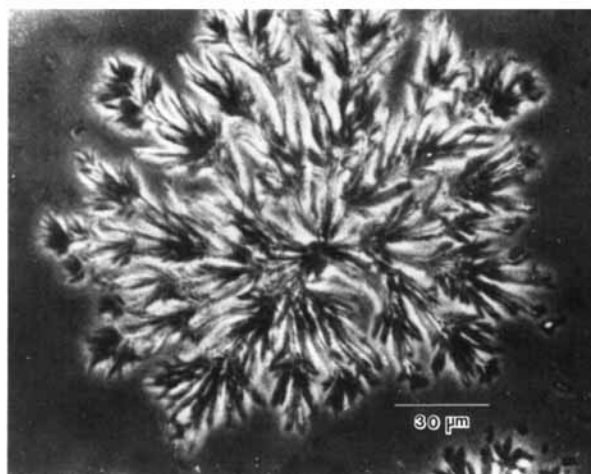
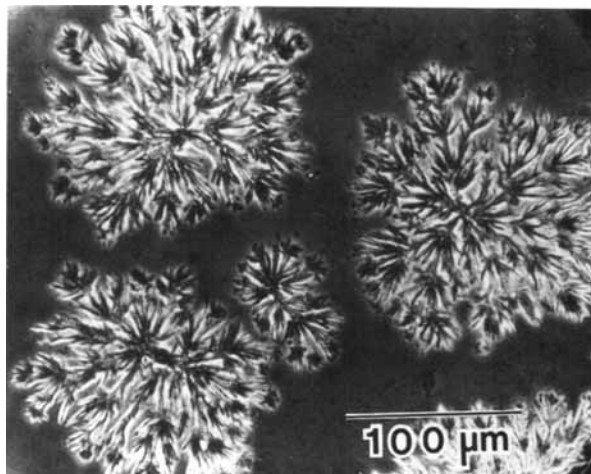


**Figure 14.** (a) Phase contrast light micrograph illustrating banded spherulites grown from a 15/85 blend as they appear after the PEA has been washed away. The smaller structure is a relatively immature spherulite. (b) A view at higher magnification of the spherulite on the top left-hand side of the field in (a). Note the radially periodic "spurts" of fan-like branching, see text.

The light and electron micrographs shown in Figures 16–18 were obtained from banded spherulites grown from a 15/85 blend crystallized at 145°C in which the band period was about 25 μm. Figure 16 illustrates such spherulites as seen with phase contrast light microscopy after the PEA was washed away. Recurring spurts of branching characteristic of the proliferation of radial growth in the spherulites along all azimuths are discernible in this micrograph. The scanning electron micrograph shown in Figure 17 evidences in outline a prevailing azimuthally in-phase alternation in the radial texture of the spherulite. The morphological characteristics

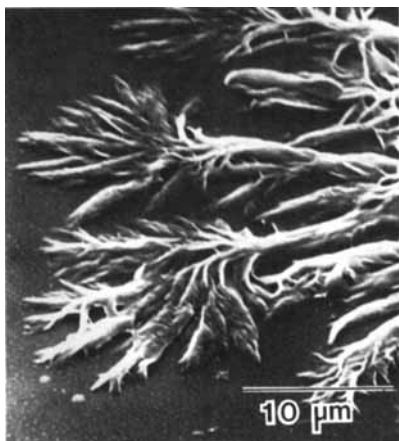


**Figure 15.** Scanning electron micrograph of a portion of the periphery of a spherulite grown from a 15/85 blend at 150°C.

that underlie the 25- $\mu\text{m}$  radially periodic changes in textural appearance are illustrated in more detail in Figure 18, which is a transmission electron micrograph of a replica of a region in the interior of a spherulite. It can be seen from Figures 16–18 (as well as Figures 14 and 15) that the outward proliferation of growth in the spherulites is characterized by the following distinctly repetitive pattern of propagation. The dominant alternating features of the pattern are the radial development of discrete, seemingly trunk-like segments of growth (macrobranches), and the somewhat abrupt fan-like splaying which these segments undergo. Upon further growth the pattern is repeated with the splayed lamellae developing outwards as discrete trunk-like segments (macrobranches) which in turn undergo

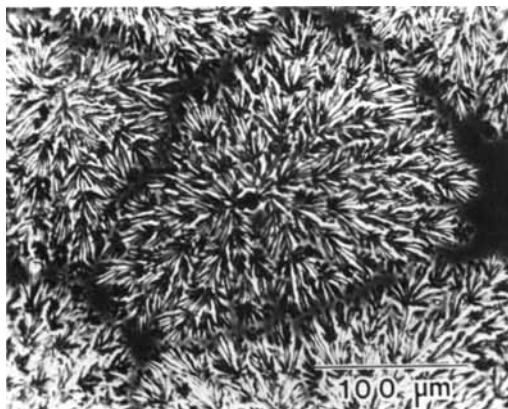


**Figure 16.** Phase contrast light micrograph illustrating banded spherulites grown from a 15/85 blend at 145°C as they appear after the PEA has been washed away.

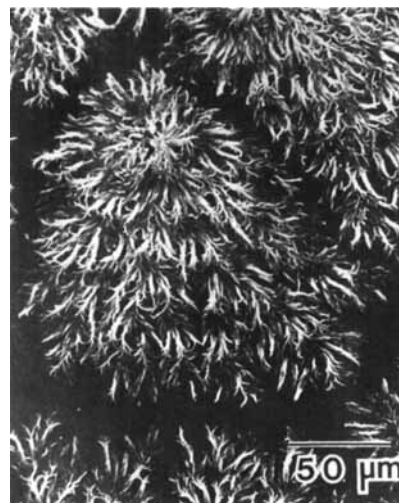


**Figure 17.** Scanning electron micrograph of a spherulite grown from a 15/85 blend at 145°C. Note the azimuthally in-phase alternation in the radial texture of the spherulite (see text).

fan-like splaying, and so forth. A simplified schematic representation, in plan view, of this repetitive process is shown in Figure 19. Observations on details of the lamellar texture which underlie the recurring radial pattern of growth depicted in the latter figure are described below.

A transmission electron micrograph of the replica of a region in the interior of a spherulite from the same preparation as that from which Figures 16–18 were obtained, is shown in Figure 20. This figure illustrates the lamellar texture in part of a dominant macrobranch L1-L2 and its associated fan-like splaying L3. Interleaved lamellar layers oriented with their long axis ( $b$  axis) preferentially parallel to the long axis of the branch may be seen in region L1 where they are also oriented preferentially flat-on in the field of view. This latter orientation contrasts with region L2 further along the branch. As would be expected of propagation from region L1 to region L2 involving in effect a twisting of interleaved lamellae through approximately 90° about their preferred direction of growth, closely spaced steps can be seen in region L2 running parallel to the length of the branch and leading to the region L3 of fan-like splayed lamellae.

A transmission electron micrograph of a replica of a portion of another spherulite from the same preparation as Figure 20 is shown in Figure 21. Included in this micrograph are several trunk-like, or incipiently trunk-like, branches (for example M, N, P, Q), which have emerged radially from a region

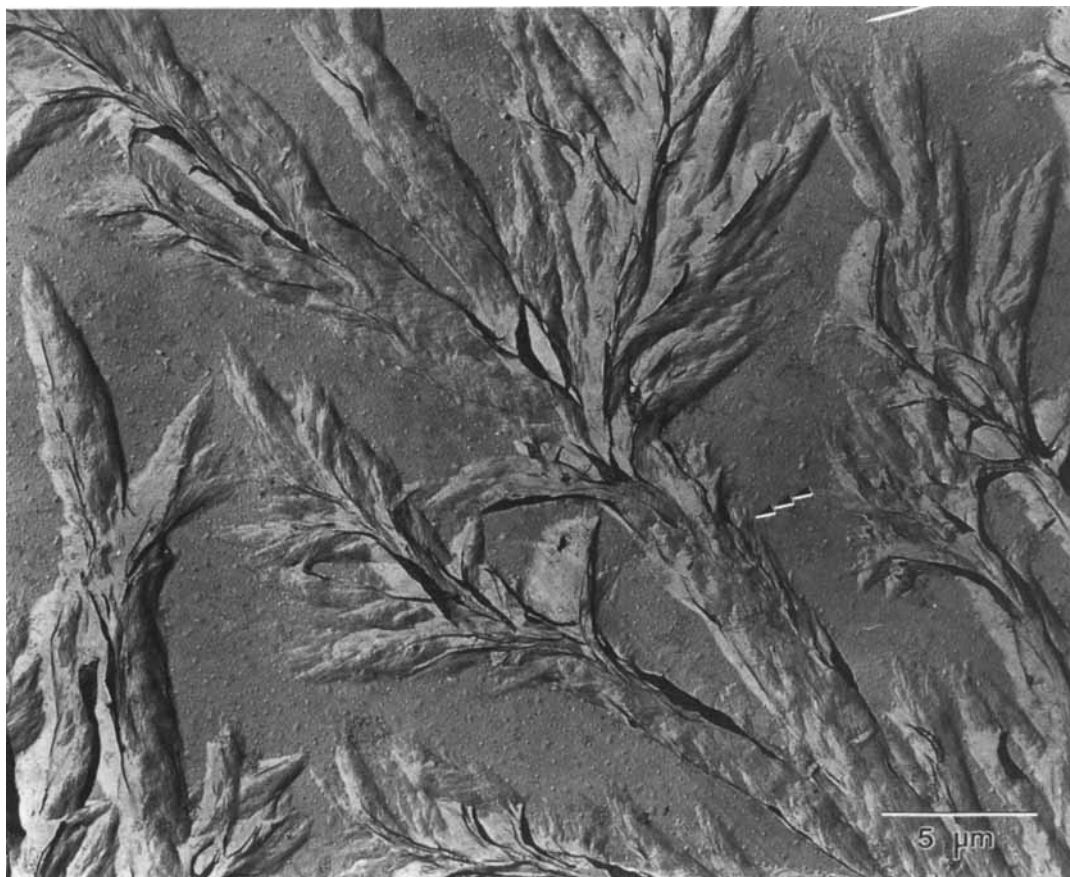


**Figure 18.** Transmission electron micrograph of a replica of a region in the interior of a spherulite grown from a 15/85 blend at 145°C illustrating the growth pattern that underlies the banding in the spherulites. Note the discrete trunk-like branch (barbed arrow) and the fan-like splaying of lamellae that has emerged therefrom.

of fan-like splaying whose center lies out of the field of view shown, and well below the midpoint of the lower edge of the picture. Considering branches M, N, P, and Q in Figure 21, attention is drawn to the regions M1, N1, P1, and Q1 along these branches where the tips of lamellae can be discerned and where the constituent interleaved lamellae at the surface of the branches are oriented preferentially parallel to the plane of the field of view. Proceeding further along the branches, a surface texture of closely spaced steps running parallel or at a small angle to the growth direction can be seen in regions M2, N2, P2, and Q2, respectively. These observations may be reasonably adduced as evidence that twisting about the outward direction of propagation is a feature that underlies the growth of the developing macrobranches.

In summary, the foregoing observations (Figures 14–21) on the banded spherulites grown from 15/85 blends indicate that while twisting of interleaved

lamellae about the  $b$  axis underlies the radial propagation of growth and the banding in these spherulites, the periodicity of the radial changes in orientation they exhibit is distinctly characterized by a repetitive pattern of growth or *motif* involving the radial propagation of twisting lamellae coupled to a correspondingly periodic manifestation of fan-like lamellar splaying. There is an evident kinship between the coupled elements of lamellar twisting and fan-like splaying that dominate the morphological development of the aggregates grown from the 5/95 blends (Figures 5–13), and the motif whose repetitiveness governs the radial propagation of growth and the manifestation of banding in the spherulites described above. The openness of the texture of the banded spherulites grown from the 15/85 blend, which openness is particularly evident away from their central region, is such that the recurring development of the twisting/splaying motif along different radial paths occurs independently of

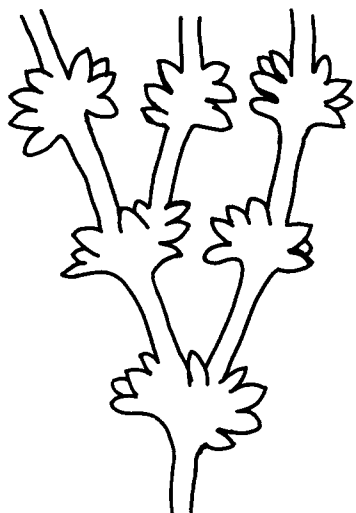


**Figure 19.** Schematic representation of the repetitive growth pattern that underlies the manifestation of banding in PVF<sub>2</sub> spherulites grown from PVF<sub>2</sub>/PEA blends. The main alternating features of the pattern are the radial development of discrete trunk-like growth segments ("macrobranches," see text) consisting of stacked interleaved lamellae, and the somewhat abrupt fan-like splaying of lamellae therefrom. Upon further growth, the latter lamellae evolve into macrobranches which in turn undergo splaying, and so forth.

growth in adjoining paths, as conveyed schematically in Figure 19. The spatial periodicity of the motif in the radial direction, which becomes shorter with decreasing crystallization temperature, and the in-phase radial recurrence of the motif along different radial paths are apparently not governed by cooperative influences of a lock-in step nature between laterally adjacent macrobranches or their associated fanned lamellae in these open textured spherulites.

## DISCUSSION

This section consists of two parts. First, the differences in lateral growth habit between the basically lozenge-shaped lamellae grown from the PVF<sub>2</sub>/PEA blends, as compared to the quasi-hexagonal lateral growth habits exhibited by  $\alpha$ -PVF<sub>2</sub> lamellar crystals grown from dilute solutions in 9 : 1 MCB/DMF,<sup>6-9</sup> is briefly discussed. Second, some considerations and speculations are presented concerning the origins of the coupled lamellar twisting/fan-like splaying characteristics that govern the growth of the aggregates formed from the 5/95 blends and the radial periodicity of the banding in the spherulites grown from the 15/85 blends.

### On the Differences in the Lateral Growth Faces Exhibited by $\alpha$ -PVF<sub>2</sub> Crystals

Systematic changes in the lateral growth habits of solution-grown polymer crystals reflecting changes in the relative growth rates of different crystal faces with crystallization temperature, undercooling, solvent, polymer concentration, and molecular weight are well known in the case of polyethylene (e.g., see bibliography in ref. 14). The effects of temperature and polymer concentration on the lateral growth habits of polyethylene crystals grown from xylene<sup>14</sup> have been analyzed in detail in terms of the kinetic theory of polymer crystal growth.<sup>15</sup> As indicated in that analysis, changes in the relative growth rates of different crystal faces relative to one another imply that the parameters that control the growth rates, principally the lateral and fold surface free energies, are different. In addition, these surface energies may also be affected differently by temperature and polymer concentration. Similar considerations arise with regard to the differences in lateral growth habits and faceting characteristics between the present  $\alpha$ -PVF<sub>2</sub> crystals grown from PVF<sub>2</sub>/PEA blends as compared to the well-defined near-hexagonal and the quasi-hexagonal shaped  $\alpha$  crystals grown from 9 : 1 MCB/DMF.<sup>6-9</sup>

The lateral growth habit exhibited by the lozenge-shaped lamellar crystals of  $\alpha$ -PVF<sub>2</sub> grown from the 0.5/99.5 blend at 150°C, and whose chain-folded layers are bounded by {110} growth faces (Figures 2 and 3), is prototypical of the lateral habits of all the  $\alpha$ -PVF<sub>2</sub> crystalline lamellae grown from PVF<sub>2</sub>/PEA blends in this study. The dendritic lateral habits with enhanced growth parallel to the *b* axis, which are exhibited by the crystals grown from the 0.5/99.5 blends at 135°C, and by the constituent lamellae in the aggregates and banded spherulites grown from the blends having higher PVF<sub>2</sub> concentrations, derive from the {110} faceted lozenge habit. No (020) faceting in lamellae was observed in the temperature and concentration range covered in the present experiments.

Where they have been clearly specified, the crystallization conditions used in the previous studies of crystals grown from 9 : 1 MCB/DMF<sup>6-9</sup> are described as being similar to the conditions originally adopted by Okuda et al.<sup>6</sup> These authors pointed out that the polymer is soluble in this mixed solvent above 130°C. The polymer concentration was 0.01 or 0.1% and crystallization was carried out by slowly cooling (rates unspecified) the solutions. Thus, in addition to the different solvent system, and the lower polymer concentrations used, the crystals

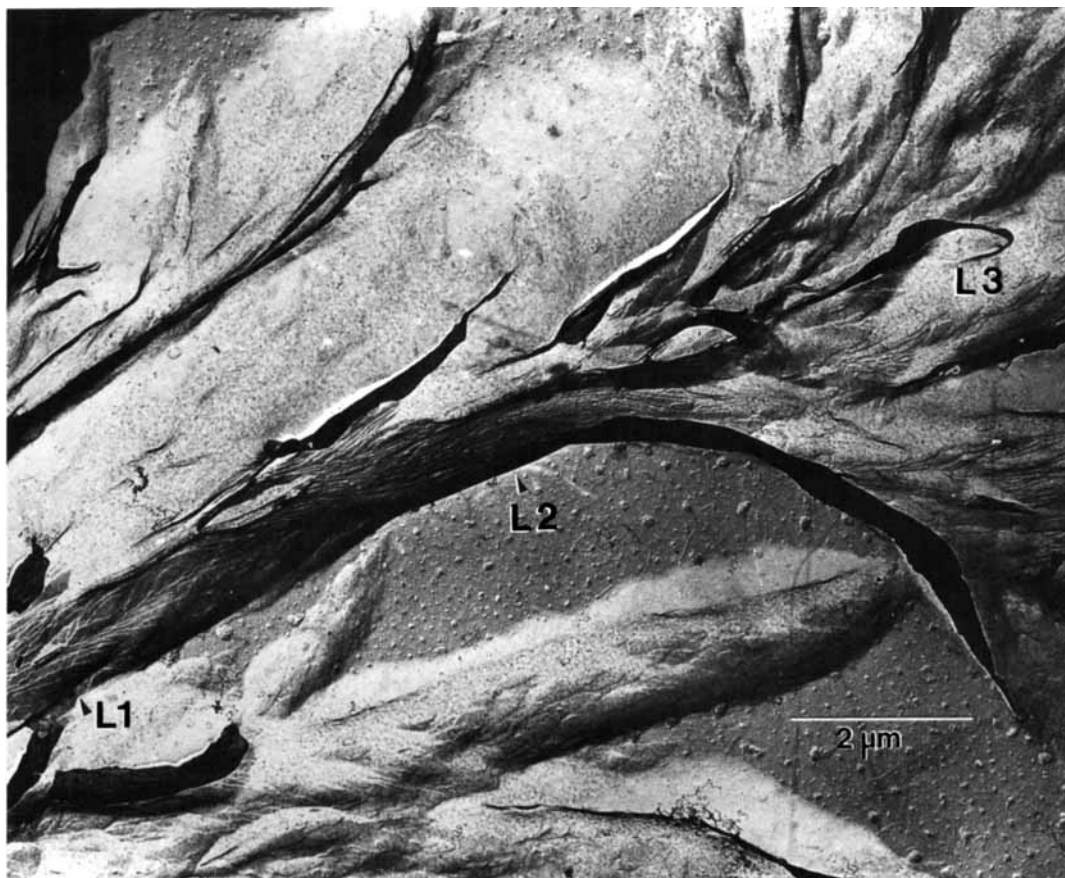


**Figure 20.** Transmission electron micrograph of a replica of a region in the interior of a spherulite grown at 145°C from a 15/85 blend. The image illustrates a radially oriented macrobranch L1-L2 and the coupled manifestation of the fan-like splaying of lamellae L3.

grown in these studies were formed under non-isothermal conditions and at lower temperatures (< 130°C) than in the present study. Furthermore, whereas some of the crystals grown from MCB/DMF exhibited distinct {110} and (020) growth faces, others exhibited variously rounded profiles. This multiplicity of variables precludes at present any meaningful assessment of the origins of the differences in lateral growth habit between the crystals grown from the PVF<sub>2</sub>/PEA blends, as compared to those grown from 9 : 1 MCB/DMF. Some considerations, pertinent to future probings of these differences, are presented below with reference to the schematic illustrations in Figure 22a,b.

Referring to the near hexagonal crystal habit depicted in Fig. 22a, let  $G(110)$  and  $G(020)$  be the growth rates normal to the {110} and (020) faces respectively. Both rates may be assumed to be constant in time at a given temperature, other factors (polymer molecular weight, concentration) being equal.<sup>14,15</sup> Let  $W(a)$  and  $W(b)$  be the lengths of the

crystal in the  $a$  and  $b$  axis directions, respectively. The habit of the crystal can be characterized in terms of the *aspect ratio*  $R = W(b)/W(a) = [G(020)]/[G(110)/\cos \phi]$ , where  $\phi = 27.2^\circ$  is the angle between the normal to a {110} face and the  $a$ -axis direction. The aspect ratio of the lozenge habit in Figure 22b is  $R(1) = b/a = 1.944$ , namely the ratio of the magnitudes of the  $b$  (= 0.964 nm) and the  $a$  (= 0.496 nm) axes of the  $\alpha$ -PVF<sub>2</sub> unit cell.<sup>2</sup> As can be visualized from Figure 22, increases in  $G(020)$  relative to  $G(110)$  will result in a progressive transition in habit from that depicted in Figure 22a to that in 22b and is characterized by increases in  $R$  and decreases in the length of the (020) faces relative to the {110} faces. By analogy with the previously referred to analysis of the habits of polyethylene crystals grown from xylene,<sup>14</sup> the absence of (020) faceting in  $\alpha$ -PVF<sub>2</sub> lamellae grown from the PVF<sub>2</sub>/PEA blends may be adduced as evidence that under the circumstances  $G(020)$  is sufficiently greater than  $G(110)$  that incipient (020)

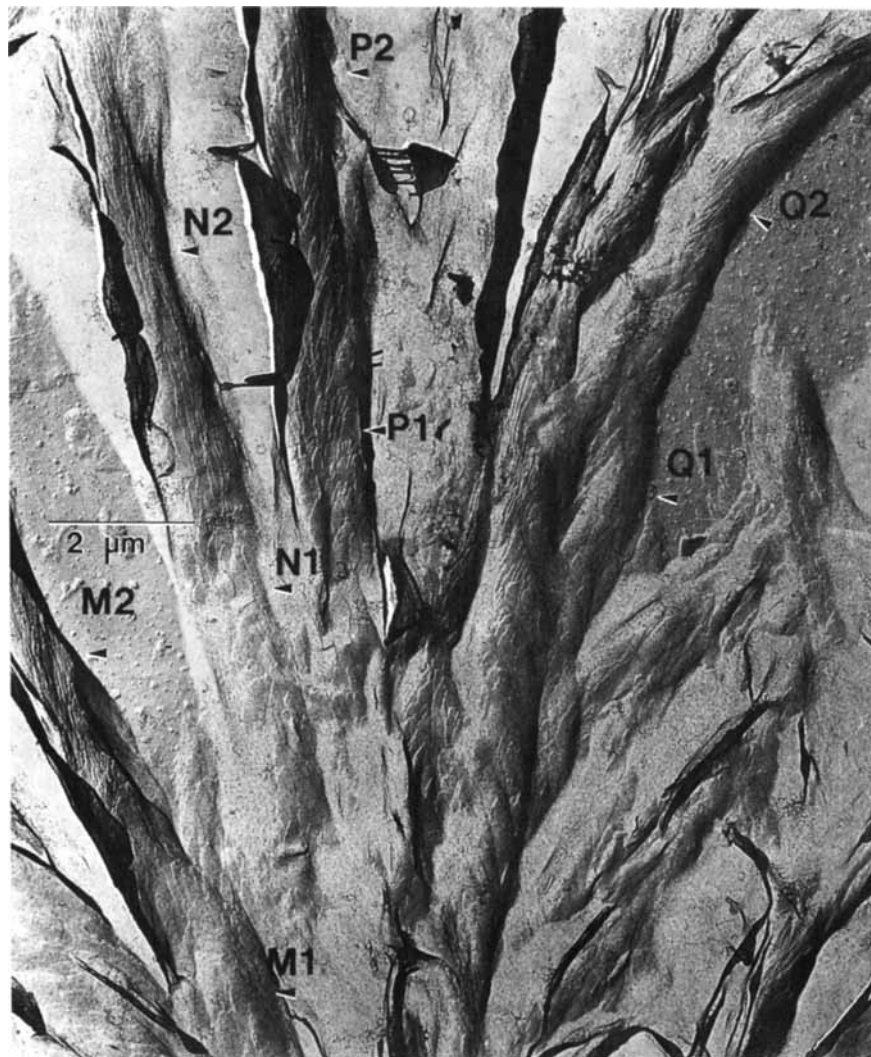


**Figure 21.** Transmission electron micrograph of a replica of a region in the interior of a spherulite grown at 145°C from a 15/85 blend, illustrating several trunk-like or incipient trunk-like macrobranches (see text) denoted M, N, P, and Q. These branches have emerged from a region of fan-like splaying centered well below the midpoint of the lower edge of the picture.

faces “grow” out of the crystal and never develop. In this view, chain-folding along (020) planes will not develop when  $G(020)/G(110)$  closely approaches and equals  $\text{cosec } \phi (= 2.19)$ , at which limit  $R = R(1)$ .

The establishment of distinct trends in changes of the ratio  $G(020)/G(110)$  as a function of crystallization conditions would provide more rigorous grounds for resolving the origins of the diversities in the lateral growth habits of  $\alpha$ -PVF<sub>2</sub> crystals. On the face of the available phenomenological data, a systematic study of the effects of concentration and temperature (as well as supercooling) under *isothermal conditions of crystallization* on the lateral

habits of crystals grown from the 9 : 1 MCB/DMF would be particularly interesting in this regard. It should at least shed some light on the causes of the rounded lateral shapes exhibited by crystals illustrated in previous studies.<sup>6-9</sup> Indeed, these variations in shape suggest in themselves variations in  $G(020)/G(110)$  under the prevailing nonisothermal crystallization conditions. As for  $\alpha$ -crystal growth from PVF<sub>2</sub>/PEA blends, the present study indicates that if (020) faceting occurs at all, evidence of its manifestation should be sought at PVF<sub>2</sub> concentrations lower than the 0.5/99.5 composition, and at lower crystallization temperatures than 135°C.

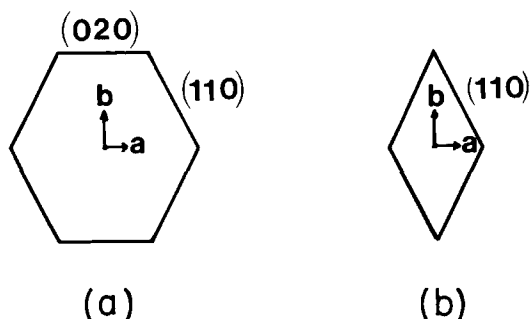


**Figure 22.** Schematic representation of (a) an  $\alpha$ -PVF<sub>2</sub> crystal bounded by {110} and (020) lateral growth faces and (b) a crystal bounded by {110} faces.

**On the Origins and Implications of the Composite Lamellar Twisting and Splaying Characteristics Which Govern the Morphological Development of the  $\alpha$ -PVF<sub>2</sub> Aggregates (5/95 Blends) and the Banded Spherulites (15/85 Blends)**

The planar conformation of the lozenge shaped (Figures 2 and 3) and the dendritic (Figure 4) lamellar crystals grown from the 0.5/99.5 blend at 150 and 135°C, respectively, contrasts with the complex lamellar growth characteristics exhibited by the aggregates (5/95 blend, Figures 5–13) and the banded spherulites (15/85 blend, Figures 14–21). The observations described in previous sections indicate that a basically similar type of growth motif governs the morphological development of the aggregates and the banded spherulites. The dominant features of this motif are growth involving the twisting of the orientation of lamellae about the *b*-axis direction, leading on to a coupled manifestation of fan-like splaying. The specificity of the coupling of these two features is vividly evidenced in the spherulites in which the repeat period of the motif corresponds to the crystallization-temperature dependent spacing between extinction bands. Although many details of the structure and morphology of the aggregates and the spherulites remain to be resolved, the present results provide a sufficient basis for outlining in broad terms pertinent considerations regarding the origins of the type of composite twisting/fan-like splaying lamellar growth and propagation characteristics at hand.

Stresses at the fold surfaces induced by the bulkiness of chain folds and/or disorder at these surfaces due to irregular folding have been invoked as the root cause of the twisting of lamellae in banded polymer spherulites.<sup>16,17</sup> In the early model due to Hoffman and Lauritzen,<sup>16</sup> the twisting of a lamella

was likened to that of a heated symmetrical trimetallic strip twisting under the influence of surface stresses that were implicitly assumed to be equal at opposite surfaces. More recently, in a detailed effort to account for the twisting and other conformational characteristics of the lamellae in banded spherulites of polyethylene determined in large measure by Bassett et al.,<sup>18–21</sup> Keith and Padden<sup>17</sup> proposed that unequal stresses at opposite fold surfaces of individual lamellae are the root cause of lamellar twisting in banded polymer spherulites. Briefly, Keith and Padden<sup>17</sup> postulated that unequal stresses at opposite fold surfaces of a chain-folded lamella arise when the lateral growth faces and the fold surfaces of a lamellar crystal are not orthogonal, that is, when the chain stems are tilted appreciably with respect to the lamellar normal, as is the case in polyethylene. More recently, Keith et al.<sup>23</sup> have presented evidence supporting this interpretation of how axial torques giving rise to twisting may arise in radially oriented lamellae in polyethylene spherulites.

Whether a tilting of the chain stems, such as envisaged by Keith and Padden,<sup>17</sup> occurs in the lamellae in the banded PVF<sub>2</sub> spherulites grown from the 15/85 blends and the aggregates grown from the 5/95 blends, remains to be determined. For this purpose, crystallization will have to be carried out in much thinner films than prepared in the present study to permit electron diffraction experiments. Clearly, any tilting of the chain stems relative to the normal to the fold surfaces of the lamellae in the PVF<sub>2</sub> aggregates and the spherulites would contrast with the results obtained for the crystals grown from the 0.5/99.5 blend (Figure 3). Stem tilting at the higher PVF<sub>2</sub> concentrations could, however, be reasonably rationalized in terms of fold staggering, which relieves overcrowding at the fold surfaces due to less regular (bulkier) chain folding at the prevailing higher growth rates. In any event, it can be reasonably presumed that intralamellar stresses arising at the fold surfaces as a consequence of less regular folding are a root cause of the twisting of the orientation of lamellae in the aggregates and the spherulites. Still, resolution of the phenomenon at hand is compounded by the need to account not only for lamellar twisting but for the associated occurrence of fan-like splaying. The causes of this feature remain to be resolved. Some considerations bearing on its origins are advanced below.

Viewing the fan-like splaying from the perspective of its radially periodic recurrence in the spherulites suggests that the periodicity is governed by a repetitive pattern of stress buildup and release. This may be envisaged as follows. A cumulative buildup

of stresses occurs within the twisting stack of lamellae in a developing macrobranch until a level is reached that gives rise to unsustainable conformational instabilities in the stacked lamellae, whereupon a change in propagational habit (i.e., fan-like splaying) is induced at the extremity of the macrobranch. Following the onset of the "foliating" process of splaying, there occurs a transient diminution of stresses acting upon the developing and less confined splayed lamellae. The latter lamellae retain an element of twisting due to the aforementioned intrinsically intralamellar surface stresses. In turn, there ensues a recurrence of stress buildup in the process of development of a new macrobranch from a dominant lamella (or small stack among the splayed lamellae) leading to a repetition of splaying, and so forth.

An important consideration in regard to a resolution of the causes of the fan-like splaying of lamellae is whether periodic fan-like splaying is also an underlying characteristic of the banding in PVF<sub>2</sub>  $\alpha$ -spherulites grown from undiluted polymer. This query bears importantly on the ultimate determination of whether the fan-like splaying (in association with lamellar twisting) in the aggregates and the spherulites grown from the PVF<sub>2</sub>/PEA blends is rooted in effects associated with the segregation of the noncrystallizable polymer component of the blend. A twisting/splaying motif has apparently not been observed, or resolved, as underlying the banding in PVF<sub>2</sub>  $\alpha$ -spherulites grown from undiluted polymer in earlier studies,<sup>3,4</sup> or in banded spherulites grown from PVF<sub>2</sub>/PMMA blends.<sup>4</sup> It is, however, interesting that in a recent brief report of the results of a study of banded  $\alpha$ -spherulites of PVF<sub>2</sub> grown from undiluted polymer melt, Vaughan and Bassett<sup>22</sup> indicate that the lamellae in those spherulites "do not adopt a smoothly twisted conformation but rather undergo major reorientations at regular intervals" (Fig. 38 in ref. 22). Whether the results of the present study have any bearing on this latter feature, or whether the motif at hand bears any relationship to the intriguing quasi-circular lamellar aggregates observed by Lovinger (Fig. 14 in ref. 3) near the edges of very thin melt grown  $\alpha$ -spherulites, remain matters which need to be investigated in more detail. In short, pending more detailed examinations of the morphological underpinnings of banding in  $\alpha$ -spherulites grown from undiluted polymer and from PVF<sub>2</sub> blended with other polymers (including a reexamination of the PVF<sub>2</sub>/PMMA system), the relevance of the twisting/splaying motif revealed in the present work to banding in  $\alpha$ -spherulites of PVF<sub>2</sub> more broadly re-

mains an open question. It is pertinent to point out that Hahn et al.<sup>24,25</sup> have reported that the results of small-angle x-ray diffraction absolute intensity measurements<sup>23</sup> and dielectric relaxation experiments<sup>24</sup> on partially crystalline blends of PVF<sub>2</sub> and noncrystallizable PMMA give evidence of amorphous interlamellar regions that consist of two phases: an amorphous PVF<sub>2</sub> phase and a homogeneously mixed PVF<sub>2</sub>/PMMA amorphous phase. Similar probings of any interlamellar segregation of PEA in the case of crystallization from the PVF<sub>2</sub>/PEA blend system have yet to be undertaken. Clearly the role of the segregation of the noncrystallizable polymer per se in inducing the type of composite twisting/splaying growth motif remains to be elucidated.

In addition to the probing of the factors indicated above, the determination of the causes of lamellar twisting and fan-like splaying in the aggregates and spherulites described and discussed in the present study requires a more detailed resolution of the lamellar growth and proliferation processes that underlie these associated deviations from planarity. Detailed characterization of these processes is obviated by the complexity of even the aggregates formed at 155°C (Figures 5–9) from the 5/95 blend. The results of the present study indicate that the onset of deviations from the planar conformation exhibited by the crystals grown from the 0.5/99.5 blend in the range of 135–150°C can be expected in this temperature range at PVF<sub>2</sub> concentrations within the composition range of 0.5/99.5–5/95. A study of the morphology of structures grown from such PVF<sub>2</sub>/PEA blend compositions should, in combination with the present observations, prove helpful to the development of an understanding of the nature and origins of the processes that govern the morphological evolution of the aggregates and banded spherulites described in this paper.

## SUMMARY

The main novel features of the morphology of  $\alpha$ -PVF<sub>2</sub> revealed in the present study are as follows:

(a) The lamellar crystals grown from the 0.5/99.5 blend at 150°C exhibit a lozenge shaped lateral growth habit and are bounded laterally by {110} growth faces. This habit is prototypical of the dendritic lateral habits of the constituent  $\alpha$ -lamellae in the crystals grown from the 0.5/99.5 blend at 135°C and in the aggregates and banded spherulites grown from the more concentrated blends. It differs distinctly from the previously reported quasi-hexagonal

lateral growth habits exhibited by  $\alpha$  crystals grown from dilute solutions of PVF<sub>2</sub> in a 9 : 1 mixture of monochlorobenzene and dimethylformamide.<sup>6-9</sup> The better defined among the latter crystals exhibit both {110} and (020) lateral growth faces. The lamellae grown from the PVF<sub>2</sub>/PEA blends in the concentration and temperature ranges covered in the present study did not exhibit (020) growth faces. Considerations regarding future experiments aimed at resolving the origins of these differences in the lateral growth habits of  $\alpha$ -PVF<sub>2</sub> crystals are presented.

(b) In contrast with the planar conformations of the multilayered lamellar crystals grown from the 0.5/99.5 blends, a conformationally complex motif of dendritic lamellar growth and proliferation, characterized by an effective twisting of the orientation of lamellae about the *b* axis coupled with the manifestation of a fan-like splaying of lamellae about that direction, governs the morphological development of the aggregates formed from the 5/95 blends. The radial propagation of growth in the banded spherulites formed from the 15/85 blend is governed by a radially periodic repetition of a similar or related twisting/splaying growth motif. The spatial periodicity of the motif in the radial direction corresponds to that of the band period in the spherulites, which decreases with decreasing crystallization temperature. This motif differs in its distinctive fan-like splaying component from banding due to just a helicoidal twisting of the orientation of lamellae about the radial direction. It remains an open question at this juncture whether growth motifs involving lamellar twisting and fan-like splaying, such as observed in the present study, underlie the radial propagation of growth in banded  $\alpha$ -spherulites formed from undiluted PVF<sub>2</sub> or from its blends with polymers other than PEA.

## REFERENCES AND NOTES

1. R. M. Briber and F. Khoury, *Polymer*, **28**, 38 (1987).
2. M. A. Backmann and J. B. Lando, *Macromolecules*, **14**, 40 (1981).
3. A. J. Lovinger, *J. Polym. Sci., Poly. Phys. Ed.*, **18**, 793 (1980).
4. B. S. Morra and R. S. Stein, *Polym. Eng. Sci.*, **24**, 311 (1984).
5. F. Khoury and E. Passaglia, in *Treatise on Solid State Chemistry*, Vol. 3, N. B. Hannay (ed.), Plenum Press, New York, 1976, chap. 6; (a) pp. 450-453; (b) pp. 386-393.
6. K. Okuda, T. Yoshida, M. Sugita, and M. Asahina, *J. Polym. Sci.*, **B5**, 465 (1967). It should be noted that the *a* and *b* axes referred to in this earlier study are reversed in relation to the axes of the  $\alpha$ -PVF<sub>2</sub> unit cell of Bachmann and Lando.<sup>2</sup>
7. D. T. Grubb and K. W. Choi, *J. Appl. Phys.*, **52**, 5908 (1981).
8. D. T. Grubb, P. Cebe, and K. W. Choi, *Ferroelectrics*, **57**, 121 (1984).
9. A. J. Lovinger, in "Developments in Crystalline Polymers-1" (D. C. Bassett Ed.), Chapt. 5, see Fig. 11, Applied Science Publishers Inc. N.J. (1982).
10. Trade names identified in this paper are given solely for indicating the source and type of materials or instruments used. This in no way implies endorsement or recommendation by the National Institute of Standards and Technology.
11. S. Weinhold, M. H. Litt, and J. B. Lando, *Macromolecules*, **13**, 1178 (1980).
12. Y. Takahashi and H. Tadakoro, *Macromolecules*, **13**, 1317 (1980).
13. A. J. Lovinger, *Macromolecules*, **14**, 332 (1981).
14. E. Passaglia and F. Khoury, *Polymer*, **25**, 631 (1984).
15. J. D. Hoffman, G. T. Davis, and J. I. Lauritzen, Jr., in "Treatise on Solid State Chemistry", Vol. 3 (Ed. N. B. Hannay), Chapt. 7, Plenum Press, New York (1976).
16. J. D. Hoffman and J. I. Lauritzen, Jr., *J. Res. Natl. Bur. Stds.*, **65A**, 297 (1961).
17. H. D. Keith and F. J. Padden Jr., *Polymer*, **25**, 28 (1984).
18. D. C. Bassett and A. M. Hodge, *Proc. Royal Soc. Lond.*, **A377**, 25 (1981).
19. D. C. Bassett and A. M. Hodge, *Proc. Royal Soc. Lond.*, **A377**, 36 (1981).
20. D. C. Bassett and A. M. Hodge, *Proc. Royal Soc. Lond.*, **A377**, 61 (1981).
21. D. C. Bassett, *CRC Crit. Rev. Solid State Matl. Sci.*, **12**, 97 (1984).
22. A. S. Vaughan and D. C. Bassett, in *Comprehensive Polymer Science*, Vol. 2, Polymer Properties, C. Booth and C. Price, (eds.), Pergamon Press, New York, 1989, chap. 12.
23. H. D. Keith, F. J. Padden Jr., B. Lotz, and J. C. Wittmann, *Macromolecules*, **22**, 2230 (1989).
24. B. R. Hahn, O. Herrmann-Schönherr, and J. H. Wendorf, *Polymer*, **28**, 201 (1987).
25. B. R. Hahn, J. H. Wendorf, and D. Y. Yoon, *Macromolecules*, **18**, 718 (1985).

Received December 3, 1991

Revised February 24, 1993

Accepted March 30, 1993